Korean J. Chem. Eng., **24**(3), 471-476 (2007)

Mass transfer and kinetics study on the sulfite forced oxidation with manganese ion catalyst

Zhao Bo†, Li Yan, Zhuo Yuqun, Tong Huiling, Zhang Xiaowen and Chen Changhe

Key laboratory for Thermal Science and Power Engineering of Ministry of Education, Department of Thermal Engineering, Tsinghua University, Beijing 100084, China
(*Received 21 August 2006 • accepted 14 November 2006*)

Abstract–Wet limestone scrubbing is the most common flue gas desulfurization process (FGD) for control of sulfur dioxide emissions from the combustion of fossil fuels. Forced oxidation, which controls the overall reaction of the sulfur dioxide absorption, is the key path of the process. Manganese which comes from the coal is one of the catalysts during the forced oxidation process. In the present work, the two-film theory was used to analyze the sulfite forced oxidation reaction with an image boundary recognition technique, and the oxidation rate was experimentally studied by contacting pure oxygen with a sodium sulfite solution. There was a critical sulfite concentration 0.328 mol/L without catalyst or at a constant catalyst concentration value. The kinetics study focused on the active energy of the reaction and the reaction constant k; furthermore, we obtained the order with respect to the sulfite and Mn^{2+} concentrations. When the Mn^{2+} catalyst concentration was kept unchanged, the sulfite oxidation reaction rate was controlled by dual film and the reaction kinetics was first order with respect to sulfite while SO_3^{2-} concentration was below 0.328 mol/L; the sulfite oxidation reaction rate was controlled by gas film only and the reaction kinetics was zero order with respect to sulfite while SO_3^{2-} concentration over 0.328 mol/L. When SO_3^{2-} concentration was kept unchanged, the sulfite oxidation reaction rate depended on gas-liquid mass transfer and the reaction kinetics was different in various stages with respect to Mn^{2+} concentrations.

Key words: Kinetics, Forced Oxidation, Mass Transfer, Manganese Ion Catalyst

INTRODUCTION

Wet limestone scrubbing is the most common flue gas desulfurization (FGD) process for the control of sulfur dioxide emissions from coal combustion. The forced oxidation of sulfite is a topic of great interest in the research on the wet limestone flue gas desulfurization process. During this process, bubbling air passes through the sulfite solution in order to achieve the forced oxidation conditions and to improve the dewatering properties of the sludge in the scrubber loop. Under these conditions, forced oxidation of the sulfite in the holding tank solves the main problem of the disposal of the solid by-product (sludge composed of calcium sulfite and sulfate). This process in the scrubber loop improves the sludge dewatering, leading to $CaSO_4$ gypsum formation.

Forced oxidation is caused by injecting air into the liquid phase according to the following reaction:

$$HSO_3^- + \frac{1}{2}O_2 \rightarrow H^+ + SO_4^{2-} \quad (1)$$

$$SO_3^{2-} + \frac{1}{2}O_2 \rightarrow SO_4^{2-} \quad (2)$$

The kinetics of such reactions, particularly the absorption of oxygen by basic solutions of sodium sulfite in the presence of catalysts, has received much attention during the last 40 years. Studies of sulfite oxidation reaction kinetics have shown the extreme sensitivity to experimental conditions, which often prevent obtaining reproducible results. Experiments have shown that the liquid-phase composition sulfite concentration, dissolved oxygen, pH value, temperature, and even traces of catalysts (Co^{2+}, Mn^{2+}, Cu^{2+}) and inhibitors (alcohols, phenols, hydroquinone) strongly affect the reaction rate [1].

Studies of heterogeneous sulfite oxidation are commonly used in mass transfer characteristics determination in gas-liquid contactors such as stirred tank absorbers, wetted wall absorbers, sieve plates and loop reactors. Generally, the presence of chemical reactions will enhance the mass transfer across gas-liquid interface, which is the determining step of the whole mass transfer process. Therefore, it is important to describe theoretically the gas-liquid mass transfer characteristics. The gas-liquid mass transfer models, such as film theory [2], penetration theory [3], surface renewal theory [4] and film-penetration theory [5] have been widely researched in recent decades.

The study of sulfite oxidation in heterogeneous conditions has received much attention in the last 20 years, since these conditions are very similar to those encountered in FGD processes. Some of the results related to the sulfite oxidation in conditions of typical of FGD process are reported in Table 1. Studies of heterogeneous sulfite oxidation are commonly used in mass transfer characteristics determination in gas-liquid contactors such as stirred tank absorbers [13] and wetted wall absorbers [14].

In present study, the sulfite oxidation reaction rate is measured via photographic method. Experiments have been conducted to study the kinetics of the oxidation reaction for various temperatures and

†To whom correspondence should be addressed.
E-mail: bobmail98@mails.tsinghua.edu.cn
‡This work was presented at the 6th Korea-China Workshop on Clean Energy Technology held at Busan, Korea, July 4-7, 2006.

Table 1. Preview results for the sulfite oxidation kinetics in FGD conditions

Ref.	T (°C)	pH	Order in		
			$S_{(IV)}$	O_2	Mn^{2+}
[6]	40	4.6-5.0	3/2	~	~
[7]	40	<3	0	0-1	0-2
[8]	25	1-4	0-1	0	1-2
[9]	26	1.5	0	1	2
[10]	25-75	4-5	0	0-1	1/2
[11]	26	3.9-4.8	0	1	0
	26	4.8-6.6	3/2	0	1/2
[12]	26	4.5-6.0	3/2	0	1/2
	26	3.8-4.2	0	1	0

Note: "~" indicates that the dependence was not studied.

Mn^{2+} concentrations and to investigate the fundamental mechanism controlling forced oxidation. The image boundary recognition technique [15] was used, which a single oxygen bubble in the sulfite solution has been monitored by a CCD camera to measure the sulfite oxidation reaction rate. The reaction rate data are obtained by using image processing software to measure the bubble pictures.

REACTION MODEL

1. Kinetic Model

It is usually accepted that a chain reaction mechanism [16] sulfite sulfur is catalyzed by transition metal ion. The kinetics chain reaction mechanism leading to the following rate steps:

$$SO_3^{2-} + Me^{+s} \xrightarrow{k_1'} \cdot SO_3^- + Me^{+(s-1)} \quad (3)$$

$$\cdot SO_3^- + O_2 \longrightarrow \cdot SO_5^- \quad (4)$$

$$\cdot SO_5^- + SO_3^{2-} \xrightarrow{k_3'} \cdot SO_5^{2-} + \cdot SO_3^- \quad (5)$$

$$SO_5^{2-} + SO_3^{2-} \longrightarrow 2SO_4^{2-} \quad (6)$$

This mechanism, with some slight modifications, is generally accepted. Assuming that Eq. (4) is rapid and does not limit the overall reaction rate and the termination occurs primarily by the combination

$$\cdot SO_5^{2-} + \cdot SO_5^- \xrightarrow{k_5'} \text{inert products} \quad (7)$$

The values of the homogeneous sulfite oxidation reaction order with respect to the individual reacting species are summarized by Eq. (8).

$$v = k c_{SO_3^{2-}}^{3/2} c_{O_2}^{0} c_M^{1/2} \quad (8)$$

Where v is the sulfite oxidation reaction rate, k is the sulfite oxidation rate constant, $c_{SO_3^{2-}}$ is the sulfite concentration, c_{O_2} is the oxygen concentration in the gas, c_M is the catalyst concentration.

2. Mass Transfer Model

In a relatively stable condition, the two-film theory [2] is the most suitable model on the mass transfer between the gas-liquid systems. It is assumed that:

(1) There is relatively stable film between the gas and the liquid;

(2) Inter-phase mass transfer drag is zero; mass transfer resistance is concentrated in the two films;

(3) In the mid-continent region, the concentration of the gas is equal.

3. Model Analysis

Based on the two-film theory, the oxygen in the sulfite solution absorption rate could be written as Eq. (9):

$$N_{O_2} = -\frac{1}{S}\frac{dn_{O_2}}{dt} = K_{O_2,G}(p_{O_2} + \gamma C_{SO_3^{2-},L}) \quad (9)$$

where $$\gamma = \frac{1}{H_{O_2}} \cdot \frac{D_{SO_3^{2-},L}}{D_{O_2,L}} \quad (10)$$

The critical concentration is expressed in Eq. (11)

$$C_{SO_3^{2-}}^{crit} = \frac{D_{O_2,L}}{D_{SO_3^{2-},L}} \cdot \frac{k_{O_2,G}}{k_{O_2,L}} \cdot p_{O_2} \quad (11)$$

when $C_{SO_3^{2-},L} \geq C_{SO_3^{2-}}^{crit}$ $\quad N_{O_2} = k_{O_2,G} \cdot p_{O_2}$ (12)

where $C_{SO_3^{2-},L}$ is the sulfite concentration in liquid bulk, $C_{SO_3^{2-}}^{crit}$ is the critical sulfite concentration, $D_{O_2,L}$ is the oxygen diffusion constant in the liquid, $C_{SO_3^{2-},L}$ is the sulfite diffusion constant in the liquid, H_{O_2} is the henry's constant, $k_{O_2,G}$ is the oxygen mass transfer constant in the gas, $k_{O_2,L}$ is the oxygen mass transfer constant in the liquid, N_{O_2} is the absorption rate, n_{O_2} is the mole of oxygen, p_{O_2} is the partial pressure, S is the gas-liquid contact surface.

In Eq. (12), the critical concentration is determined by the diffusion coefficient, mass transfer coefficient and partial pressure of oxygen.

EXPERIMENTAL APPARATUS AND PROCEDURE

1. Apparatus

A rectangular vessel made of transparent glass was used to contain the sulfite solution. The vessel was properly sealed to prevent any contact between air and the solution. Nitrogen was added to further protect the sulfite solution from oxidization by oxygen in air. The vessel volume was about 20 L (200 mm×200 mm×500 mm). A pure oxygen bubble was generated from an orifice in the bottom plate. A gas handling system provided precise control of the oxygen flow. At the beginning of the experiment, a pure oxygen bubble was generated in the sodium sulfite solution. Experiments showed that bubbles with diameters less than 4 mm stayed intact to the orifice due to the surface tension. The oxygen was then gradually absorbed by the sulfite reaction, which reduced the bubble volume. A CCD camera (Sony DCR-TRV20E) recorded the magnified bubble image projected on a frosted glass plate, and sent the images to a computer for later analysis. Sample bubble images captured by CCD camera and the boundary identification images at different times during one reaction process are shown in Fig. 2 and Fig. 3. The image-processing software recognized the height and the bottom of the bubble and fitted the edge curve by Young-Laplace equation. After a successful fitting, the bubble volume, the interfacial area, and the radius of curvature at the top of the bubble were derived from the image-processing results. As the pure oxygen was filled in the bubble, the sulfite oxidation reaction rate was then determined from these parameters [17,18].

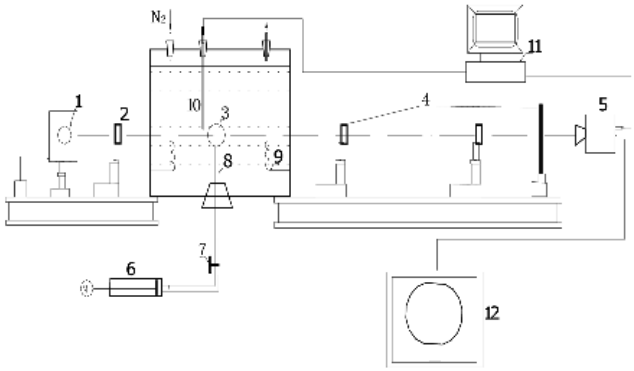

Fig. 1. Experimental apparatus.

1. Light source
2. Lens, pin holes, and filters
3. Oxygen bubble
4. Convex lenses and frosted glass
5. CCD, video camera
6. Syringe and syringe pump
7. Valve
8. Plastic tube
9. Heater
10. Thermometer
11. A/D card and PC
12. Screen of the camera

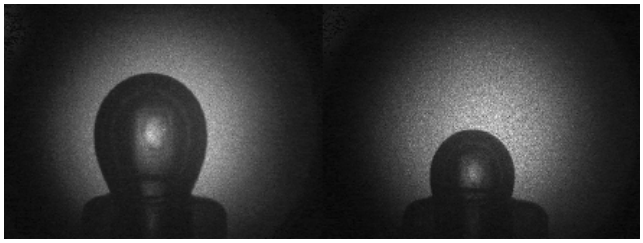

Fig. 2. Bubble images captured at 0 second and 1,080 seconds at 310 K.

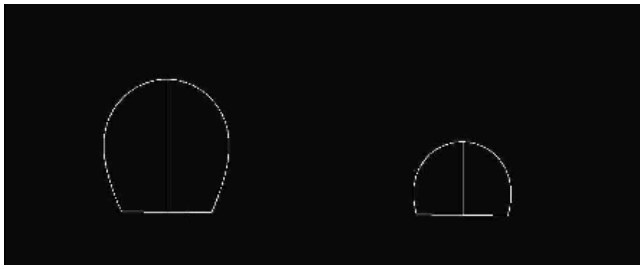

Fig. 3. Edge determined from the bubble images shown in Fig. 2.

Fig. 1 shows the test rig of the oxygen bubble generation system and the bubble image recording system.

2. Data Procedure

v is defined as the area reaction rate of sulfite oxidation, and Eqs. (13) and (14) give the numerical solution. Many researchers could only give the volume reaction rate since it was very difficult to get the exact gas-liquid contacting area. In this study, this difficulty has been removed by a simple but effective experiment method. The exact contacting area of pure oxygen bubble and sulfite solution can be measured and calculated via optical devices.

$$v = \frac{dN}{S\,dt} \tag{13}$$

$$N = \frac{p_{O_2}V}{8.31T} = \frac{(p_0 + p_l + p_s - p_v)V}{8.31T} = \frac{(p_0 + \rho gh + 2\sigma/R - p_v)V}{8.31T} \tag{14}$$

Where N is the mole of oxygen in the bubble, p_{O_2} is the pressure in the bubble, V is the bubble volume, T is the temperature, p_0 is the atmospheric pressure, p_l is the liquid pressure, p_s is surface tension pressure, p_v is vapor partial pressure, ρ is the sulfite concentration, σ is the sulfite surface tension coefficient, R is bubble radius of curvature and h is the bubble height.

RESULTS AND DISCUSSION

In an aqueous sulfite solution, forced oxidation is carried out by injecting oxygen into the liquid phase. The kinetic equation relating the sulfite oxidation rate and the reactant concentrations is:

$$v = k c_{SO_3^{2-}}^{n_1} c_{O_2}^{n_2} c_M^{n_3} \tag{15}$$

where v is the sulfite oxidation reaction rate, k is the sulfite oxidation rate constant, $c_{SO_3^{2-}}$ is the sulfite ion concentration, c_{O_2} is the oxygen concentration in the gas, c_M is the catalyst concentration, n_1 is the order of the sulfite ion reactant, n_2 is the order of the oxygen reactant, and n_3 is the order of the catalyst reactant.

1. Effect of Reaction Temperature

If the sulfite ion and oxygen concentrations are held constant, the temperature dependence of the kinetic reaction constants can be well described by the expression

$$k = A\exp\left(-\frac{E}{RT}\right) \tag{16}$$

where k is the kinetic reaction constants, k′ is the kinetics constant of the reaction, R is the ideal gas constant, T is the temperature, and E is the activation energy. Eq. (16) can be rewritten as:

$$\ln(k) = \ln(A) + \left(-\frac{E}{R}\right) \times \left(\frac{1}{T}\right) \tag{17}$$

This is a linear equation related to 1/T and ln(v). The slope (−E/R) and the intercept (ln(A)) can be calculated from a curve of the data.

The data for the sulfite oxidation reaction rate with Mn^{2+} catalyst are shown in Fig. 4 and Fig. 5. The sulfite concentration was fixed

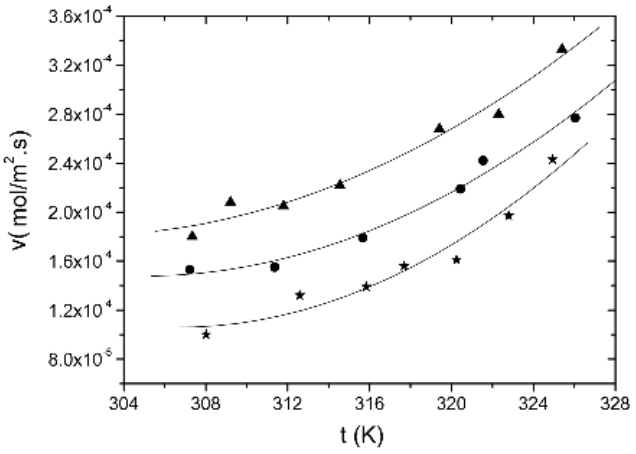

Fig. 4. Sulfite oxidation reaction rate increase with temperature.

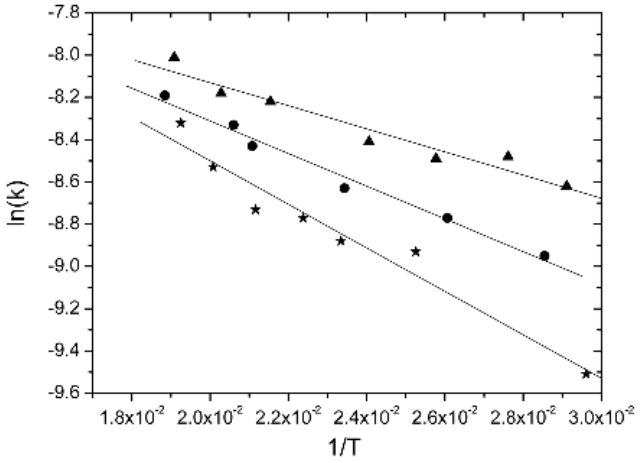

Fig. 5. Logarithm of reaction rate decrease with the reciprocal of temperature.

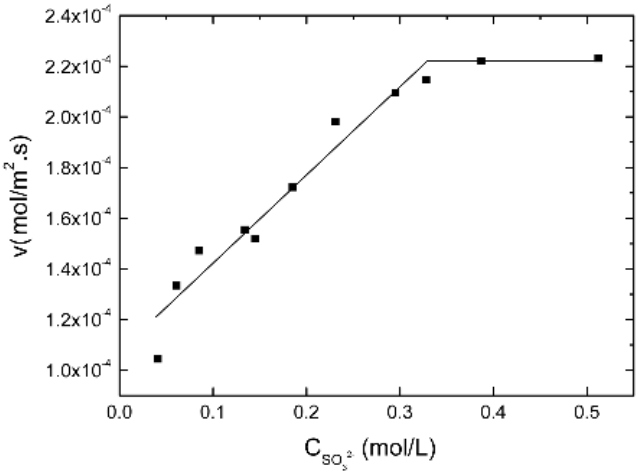

Fig. 6. Sulfite oxidation reaction rate with the sulfite ion concentration without catalyst at 320 K.

Table 2. Activation energy, preexponential factor for different Mn^{2+} concentrations

Mn^{2+} concentration (mol/L)	E (kJ/mol)	A
2.68E-04	29.38	11.02
8.88E-04	28.41	9.53
2.37E-03	25.65	9.17

at 0.085 mol/L, and the Mn^{2+} concentration in different conditions: ★ 2.68E-04 mol/L; ● 8.88E-04 mol/L; ▲ 2.37E-03 mol/L

Fig. 4 shows the trend of the reaction rate increasing with temperature, which is in good agreement with Eq. (16). So Eq. (15) could also be written as

$$v = A\exp\left(-\frac{E}{R}\right)c_{SO_3^{2-}}^{n_1}c_{O_2}^{n_2}c_M^{n_3} \quad (18)$$

Table 2 shows the activation energy E and constant A of the reaction with Mn^{2+} catalyst. The activation energy E was decreased from 29.38 kJ/mol to 25.65 kJ/mol as the Mn^{2+} concentration increased. Smaller values of E indicate heat, the reaction is easier. The sulfite oxidation reaction rate increased with temperature and Mn^{2+} concentration. In flue gas desulfurization, the temperature is limited by the system because the solubility of SO_2 in solution decreases as the temperature increases; therefore, the system has an optimum temperature. The solubility of SO_2 in solution varies little for reaction temperatures from 15-60 °C [19], but decreases rapidly for temperatures over 60 °C. Therefore, the reaction temperature should not exceed 60 °C.

2. Effect of Sulfite Concentration

Fig. 6 shows the results of the reaction rate of sulfite oxidation when the temperature is 320 K, and the concentration of the sulfite ion is changed from 0.041 mol/L to 0.512 mol/L without any catalyst.

The critical concentration of the sulfite ion $c_{SO_3^{2-}}^{crit}$ in the Fig. 6 $c_{SO_3^{2-}}^{crit}$ is presented as the limiting values above which absorption is no longer dependent on sulfite concentration. In Fig. 6 $c_{SO_3^{2-}}^{crit}$ is about 0.328 mol·L^{-1}; therefore, when $c_{SO_3^{2-}} < c_{SO_3^{2-}}^{crit}$, the reaction order relative to the sulfite ion is equal to 1, but when $c_{SO_3^{2-}} > c_{SO_3^{2-}}^{crit}$, the reaction order relative to the sulfite ion is zero.

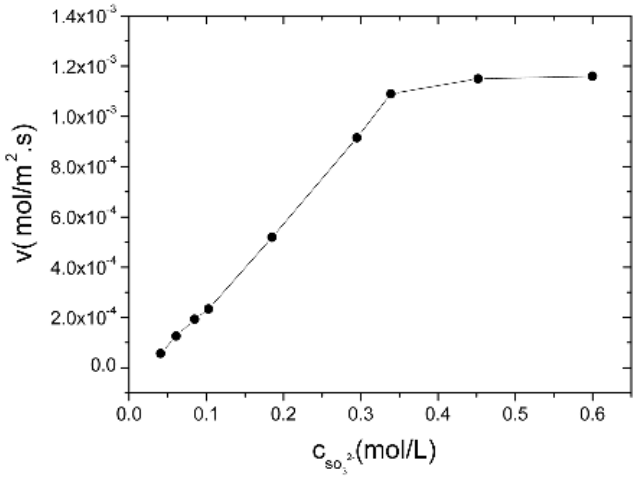

Fig. 7. Sulfite oxidation reaction rate with the sulfite ion concentration (at 320 K and Mn^{2+} concentration 1.68E-04 mol/L).

The critical sulfite ion concentration can be explained from mass-transfer characteristics of the gas-liquid system and the chemical reaction kinetics since the oxidation of the sulfite ions by the oxygen reduces the sulfite concentration near the interface with regard to the sulfite concentration in the bulk liquid phase.

Fig. 7 shows the results for the sulfite oxidation reaction rate in the presence of Mn^{2+} catalyst.

A Least Squares analysis for the data with sulfite concentration less than 0.328 mol/L showed that the reaction order with respect to the sulfite ion was 1, with a critical sulfite ion concentration of the sulfite ion $c_{SO_3^{2-}}^{crit}$ between 0.328 m/L as the limiting value above which absorption is no longer dependent on the sulfite ion concentration. This result agrees with the previous findings for $c_{SO_3^{2-}}^{crit}$ given in Table 3 [1].

3. Effect of Catalyst Concentration

Many researches found that catalysts (Co^{2+}, Mn^{2+}, etc.) strongly affect the reaction rate. The experimental results of sulfite oxidation in presence are caused by Mn^{2+} catalyst with pure oxygen. In the

Table 3. Critical sulfite concentration values given in the literature

pH	Sulfite concentration (mol\L)	T (°C)	Critical sulfite concentration (mol/L)
8	0.8	30	0.5
8.5	0.5	20	0.25
7.9	0.25	20	0.2
8.5	0.3	30	0.04
8.35	0.8	25	0.3
8.5	0.5	20	0.3
8.5	0.5	20	0.25

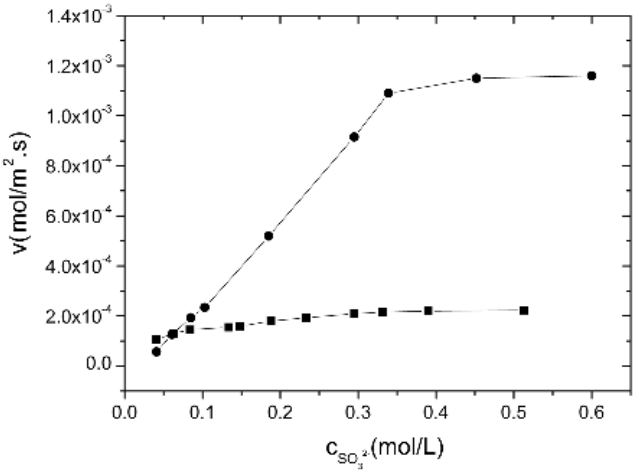

Fig. 8. Sulfite oxidation reaction rate increase with the sulfite ion concentration (at 320 K and ■ without catalyst; ● Mn^{2+} concentration 1.68E-04 mol/L).

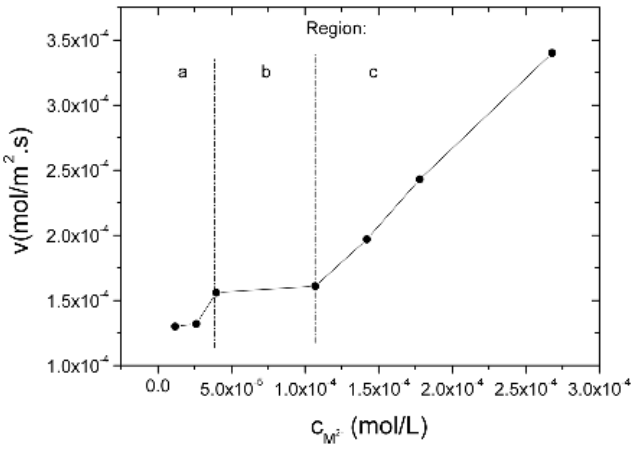

Fig. 9. Sulfite oxidation reaction rates for various catalyst concentrations (at 315 K and the sulfite ion concentration 0.085 mol/L).

first series, the total sulfite concentration was varied in the range of 0-0.6 mol/L without any catalyst. As shown in Fig. 8, the reaction rate was at a low level in the conditions of various sulfite concentrations. In the second series, the Mn^{2+} concentration was kept at 1.68E-04 mol/L; the total sulfite concentration was in the same range. The experimental results showed that Mn^{2+} enhanced the reaction rate. When the sulfite ion concentration was lower than 0.05 mol/L, the catalyst's effect was not very obvious, but the effect was stronger with the sulfite ion concentration increasing, while the Mn^{2+} concentration was even as low as 1.68E-04 mol/L, it also could enhance the reaction.

The sulfite oxidation reaction rate was shown in Fig. 9 for various Mn^{2+} catalyst concentrations and a constant temperature of 315 K and the sulfite ion concentration of 0.085 mol/L. The effect of the catalysts concentration was investigated by using Mn^{2+} concentrations from 0 to 3.0E-04 mol/L.

As the Mn^{2+} catalyst, the reaction rate can be significantly increased by solely increasing the Mn^{2+} concentration. A typical profile is shown in Fig. 9. The published results differ only in the position of the line and in the width of its regions, but the lines always follow the same shape. Linek [1] found a typical profile in which the total absorption rate of oxygen was a function of catalyst concentration. In Phase a, the reaction rate increased with catalyst concentration, with the sulfite oxidation reaction rate determined by the reaction kinetics, as a first order reaction with respect to the catalyst. In Phase b, the sulfite oxidation reaction rate was determined by mass transfer characteristics of the gas-liquid system, so the reaction order was zero. In Phase c, the reaction was very rapid with the reaction rate determined by the reaction kinetics, as a first order reaction. The reaction rate was increasing with the Mn^{2+} catalyst concentration, and the reaction went into the fast region. Therefore, the data showed that during the different phases with different catalysts concentrations, the mass transfer in the liquid phase affected the reaction rate.

4. Effect of Oxygen Concentration

In order to investigate the effect of oxygen concentration, we used simulated air composed of 21% pure oxygen and 79% pure nitrogen to perform the force oxidation experiment without any catalyst. During the bubble absorption process, we measured the original bubble size and marked oxygen concentration 21%, and then calculated oxygen concentration by the volume change.

Fig. 10 shows the sulfite oxidation reaction rate was increasing with the oxygen concentration, and the order with respect to oxy-

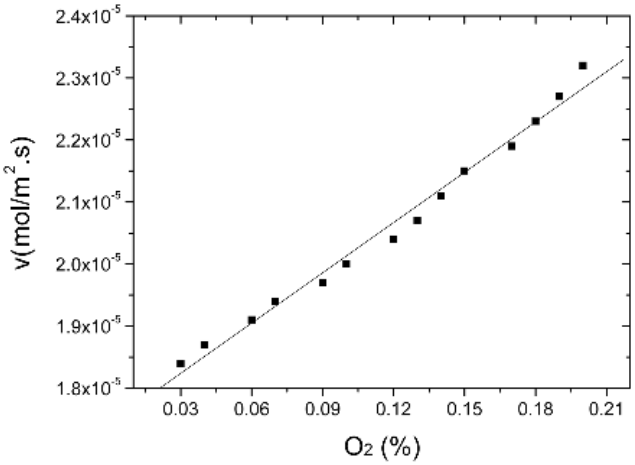

Fig. 10. Sulfite oxidation reaction rates with the oxygen concentration (at 320 K the sulfite ion concentration 0.003 mol/L).

gen concentration was 1. This result is very similar to many other researchers' findings as shown in Table 2.

As mentioned above, Figs. 6 and 7 show the results of the sulfite oxidation reaction rate against various sulfite ion concentrations without any catalyst. In this set of experiments, we used pure oxygen (99.99%) to oxidize sulfite. It has been found that the order with respect to oxygen concentration is zero when the sulfite concentration exceeds the critical value. This phenomenon could be useful in explaining the differences of some other researcher's results: the order with respect to oxygen concentration is one because the sulfite concentration is below the critical sulfite concentration, and the reaction is controlled by the kinetics. Moreover, when the sulfite concentration exceeds the critical concentration, the zero order indicates that the reaction is controlled by the mass transfer.

CONCLUSIONS

1. The experimental results show that the relation between the sulfite oxidation reaction rate and reaction temperature can be described by $v = A e^{-E/RT} c_{SO_3^{2-}}^{n_1} \cdot c_{O_2}^{n_2} c_M^{n_3}$. With the Mn^{2+} catalyst existing, the activation energy was from 25.65 to 29.38 kJ/mol, and the preexponential factor was from 9.17 to 11.02.

2. The experimental results show a critical sulfite concentration of about 0.328 mol/L, below which the reaction was first order with respect to the sulfite, and above which the order was zero.

3. The sulfite oxidation reaction rate increased with catalyst concentration, and Fig. 9 shows the trend. The sulfite oxidation reaction rate depended on gas-liquid mass transfer and the reaction kinetics was different in various stages with respect to Mn^{2+} concentrations.

4. The order with respect to oxygen concentration is different in the different sulfite condition: the order with respect to oxygen concentration is one when the sulfite concentration is below the critical concentration, and the reaction is controlled by kinetics; whilst the order is zero when the sulfite concentration is over the critical concentration, and the reaction is controlled by the mass transfer.

ACKNOWLEDGMENT

This work is supported by the State Key Development Program for Basic Research of China (2006CB200301) and by the supporting fund of the Laboratory Administration of Tsinghua University.

NOMENCLATURE

$C_{SO_3^{2-}}$: sulfite ion concentration [mol/L]
c_{O_2} : oxygen concentration in the gas [mol/L]
c_M : catalyst concentration [mol/L]
$c_{SO_3^{2-}}^{crit}$: critical sulfite concentration [mol/L]
$C_{SO_3^{2-},L}$: sulfite concentration in liquid bulk [mol/L]
$D_{O_2,L}$: oxygen diffusion constant in the liquid [m^2/s]
$C_{SO_3^{2-},L}$: sulfite diffusion constant in the liquid [m^2/s]
H_{O_2} : Henry's constant [k·Pa·kg/mol]
$k_{O_2,G}$: oxygen mass transfer constant in the gas [m/s]
$k_{O_2,L}$: oxygen mass transfer constant in the liquid [m/s]
N_{O_2} : absorption rate [mol/m^2·s]
n_{O_2} : mole of oxygen [mol]
p_{O_2} : partial pressure [Pa]
S : gas-liquid contact surface [m^2]
E : activation energy [kJ]
k : sulfite oxidation rate constant [m^3/mol·s]
A : preexponential factor [m^3/mol·s]
n_1 : order of the sulfite ion reactant
n_2 : order of the oxygen reactant
n_3 : order of the catalyst reactant
R : gas constant [J/mol·K]
T : temperature [K]
t : time [s]
v : sulfite oxidation reaction [mol/m^2·s]

Special Abbreviations
~ : sign for proportionality
- : from to

REFERENCES

1. V. Linek and V. Vacek, *Chem. Engng. Sci.*, **36**, 1747 (1981).
2. W. G. Whitman, *Chem. and Met. Eng.*, **29**, 147 (1923).
3. R. Higbie, *Trans. Am. Inst. of Chem. Eng.*, **31**, 365 (1935).
4. P. V. Danckwerts, *Ind. Eng. Chem. Res.*, **43**, 1460 (1951).
5. H. L. Toor and J. M. Marchello, *AIChE J.*, **16**, 513 (1970).
6. W. L. Weisnicht, L. Overman, C. C. Wang, H. L. Wang, J. Erwin and J. L. Hudson, *Chem. Engng Sci.*, **35**, 463 (1980).
7. W. Pasiuk-Bronikowska and T. Bronikowski, *Chem. Engng Sci.*, **36**, 215 (1981).
8. A. Jr. Huss, P. K. Lim and C. A. Eckert, *J. Phys. Chem.*, **86**, 4224 (1982).
9. W. Pasiuk-Bronikowska and J. Ziajka, *Chem. Engng Sci.*, **40**, 1567 (1985).
10. R. K. Ulrich, G. T. Rochelle and R. E. Prada, *Chem. Engng Sci.*, **41**, 2183 (1986).
11. T. Bronikowski and W. Pasiuk-Bronikowska, *Chem. Engng Sci.*, **44**, 1361 (1989).
12. J. Ziajka and W. Pasiuk-Bronikowska, *Chem. Engng Sci.*, **44**, 915 (1989).
13. A. Lancia, D. Musmarra, M. Prisciandaro and M. Tammaro, *Chem. Engng. Sci.*, **54**, 3019 (1999).
14. H. K. Lee, B. R. Deshwal and K. S. Yoo, *Korean J. Chem. Eng.*, **22**, 208 (2005).
15. B. Zhao, Y. Li, H. L. Tong, Y. Q. Zhuo, L. Zhang, J. Shi and C. H. Chen, *Chem. Engng Sci.*, **60**, 863 (2005).
16. H. L. J. Bäckström, *J. Am. Chem. Soc.*, **49**, 1460 (1927).
17. P. V. Danckwerts, *Gas-liquid reaction*, McGraw-Hill Publications, New York (1970).
18. G. C. Mishra and R. D. Srivastava, *J. Appl. Chem. Biotechnol.*, **26**, 401 (1976).
19. D. X. Shen, Z. Y. He and Y. R. Wang, *Environ. Chem.*, **12**, 99 (1993).